

Emergence of Novel Antiferromagnetic Order Intervening between Two Superconducting Phases in $\text{LaFe}(\text{As}_{1-x}\text{P}_x)\text{O}$: ^{31}P -NMR Studies

Hidekazu MUKUDA^{1*}, Fuko ENGETSU¹, Takayoshi SHIOTA¹, Kwing To LAI²,
Mitsuharu YASHIMA^{1,4}, Yoshio KITAOKA¹, Shigeki MIYASAKA^{2†}, and Setsuko TAJIMA²

¹Graduate School of Engineering Science, Osaka University, Toyonaka, Osaka 560-8531, Japan

²Graduate School of Science, Osaka University, Toyonaka, Osaka 560-0043, Japan

(Received August 27, 2018)

Systematic ^{31}P -NMR studies of $\text{LaFe}(\text{As}_{1-x}\text{P}_x)\text{O}$ compounds have revealed the emergence of a novel antiferromagnetic ordered phase (AFM-2) at $0.4 \leq x \leq 0.7$ that intervenes between two superconductivity (SC) phases. This AFM-2 phase with Néel temperature $T_N = 35$ K for $x=0.6$ is in strong contrast to the AFM order (AFM-1) at $x=0$ exhibiting T_N of 140 K. Previous ^{31}P -NMR studies of $\text{LaFe}(\text{As}_{1-x}\text{P}_x)(\text{O}_{1-y}\text{F}_y)$ have revealed that T_c reaches a maximum of 24 K for $x=0.6$ as a result of the marked enhancement of AFM spin fluctuations at low energies due to electron doping by the fluorine substitution of $y=0.05$ for oxygen. The reason for this unexpected result has been found in the present work, that is, the emergence of AFM-2 at $0.4 \leq x \leq 0.7$ without electron doping. We note that AFM spin fluctuations arising from interband nesting on the d_{XZ}/d_{YZ} orbits must be a key factor for the occurrence of SC around AFM-2.

Iron (Fe) oxypnictide LaFeAsO with an orthorhombic structure exhibits antiferromagnetic (AFM) order, and the substitution of F^- for O^{2-} induces superconductivity (SC) with a maximum transition temperature of $T_c = 26$ K in $\text{LaFeAsO}_{1-y}\text{F}_y$.¹ The isostructural compound $\text{LaFeP}(\text{O}_{1-y}\text{F}_y)$ with P substituted for As also reveals the SC transition at $T_c = 4 - 7$ K, which is lower than that in the case of $\text{LaFeAs}(\text{O},\text{F})$.² In Fe-pnictide superconductors, T_c reaches a maximum of 55 K^{3,4} when a FeAs_4 block forms a nearly regular tetrahedral structure.⁵ The optimal values of the As-Fe-As bonding angle (α), the height of pnictogen (h_{Pn}) from the Fe plane, and the a -axis length (a) are 109.5° ,⁵ ~ 1.38 Å,⁶ and ~ 3.9 Å,⁴ respectively. In this context, since the substitution of P for As makes the a -axis length smaller, α wider, and h_{Pn} smaller than the optimal values for high- T_c Fe pnictides, it is anticipated that T_c might decrease monotonically as x increases in solid solution compounds $\text{LaFe}(\text{As}_{1-x}\text{P}_x)(\text{O}_{1-y}\text{F}_y)$. Unexpectedly, T_c exhibits a nonmonotonic variation with x in $\text{LaFe}(\text{As}_{1-x}\text{P}_x)(\text{O}_{1-y}\text{F}_y)$ compounds.⁷⁻⁹ Previous ^{31}P -NMR studies of these compounds have revealed that T_c reaches its respective maxima of 27 and 24 K for $x=0.4$ with $y=0.1$ and for $x=0.6$ with $y=0.05$, as a result of the marked enhancement of AFM spin fluctuations (AFMSFs) at low energies.¹⁰ The result provides clear evidence that T_c is enhanced by AFMSFs at low energies even though the lattice parameters deviate from their optimum values. However, another question should be addressed: Why are AFMSFs enhanced despite the fact that the lattice parameters of the compounds are far from those of the AFM mother compound LaFeAsO .

In this Letter, we report the results of our ^{31}P -NMR studies that a novel AFM ordered phase (AFM-2) emerges at $0.4 \leq x \leq 0.7$, intervening between two SC phases (SC-1 and SC-2) in $\text{LaFe}(\text{As}_{1-x}\text{P}_x)\text{O}$. The ^{31}P -

NMR Knight shift indicates the appearance of a sharp density of states (DOS) at the Fermi level derived from a $d_{3Z^2-r^2}$ orbit, which is less relevant with the onset of SC-2. On the other hand, AFMSFs arising from interband nesting on d_{XZ}/d_{YZ} orbits are mainly responsible for the occurrence of SC around AFM-2.

Polycrystalline samples of $\text{LaFe}(\text{As}_{1-x}\text{P}_x)\text{O}$ were synthesized by the solid-state reaction method.^{7-9,11} Powder X-ray diffraction measurements indicated that the lattice parameters of $\text{LaFe}(\text{As}_{1-x}\text{P}_x)\text{O}$ exhibit a monotonic variation with x .¹¹ ^{31}P -NMR ($I=1/2$) measurement was performed on coarse powder samples of $\text{LaFe}(\text{As}_{1-x}\text{P}_x)\text{O}$ with nominal contents $x=0.3, 0.4, 0.5, 0.6, 0.7, 0.8$, and 1.0. The ^{31}P -NMR spectra in the AFM ordered state were obtained by sweeping a magnetic field at a fixed frequency $f_0 = 107$ MHz. The Knight shift K in the normal state was measured at a magnetic field of ~ 11.95 T, which was calibrated using a resonance field of ^{31}P in H_3PO_4 . The nuclear spin lattice relaxation rate ($1/T_1$) of ^{31}P -NMR was obtained at a field of ~ 11.95 T by fitting a recovery curve for ^{31}P nuclear magnetization to a single exponential function, $m(t) \equiv (M_0 - M(t))/M_0 = \exp(-t/T_1)$. Here, M_0 and $M(t)$ are the nuclear magnetizations for a thermal equilibrium condition and at time t after a saturation pulse, respectively.

Figure 1(a) shows the temperature (T) dependence of the ^{31}P -NMR spectrum at $x=0.6$, which exhibits significant broadening below 35 K. At 4.2 K, the ^{31}P -NMR spectrum indicates a rectangle-like spectral shape, which is characteristic of a randomly oriented powder where a commensurate AFM order takes place.¹² The ^{31}P nucleus experiences a uniform off-diagonal internal hyperfine field, $^{31}H_{\text{int}}$, associated with a stripe-type AFM order of Fe-3d spins.¹³ Actually, the spectrum can be simulated by assuming $^{31}H_{\text{int}} \simeq 0.12 \pm 0.05$ T at 4.2 K, as shown by the solid curve in Fig. 1(a). By using the relation $^iH_{\text{int}} = ^iA_{\text{hf}} M_{\text{AFM}}$, an AFM moment M_{AFM} at the Fe site is estimated to be $\sim 0.18 (\pm 0.07) \mu_B$

*E-mail: mukuda@mp.es.osaka-u.ac.jp

†E-mail: miyasaki@phys.sci.osaka-u.ac.jp

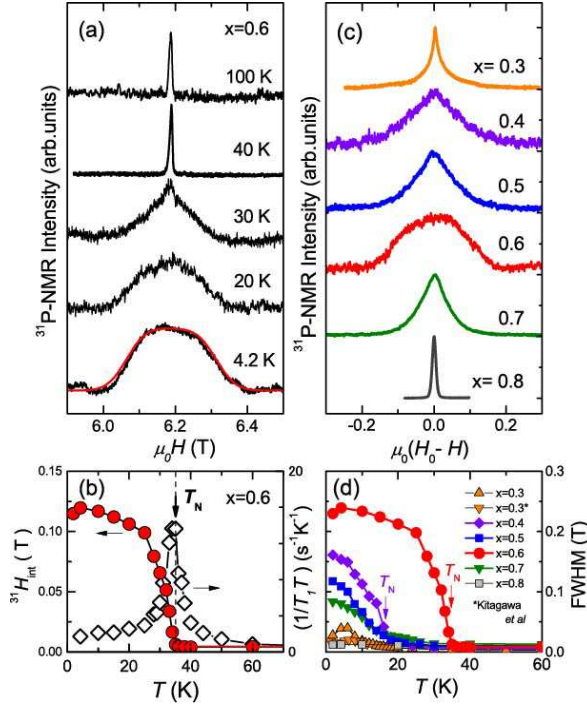


Fig. 1. (Color online) (a) T dependence of ^{31}P -NMR spectra at $x=0.6$ of $\text{LaFe}(\text{As}_{1-x}\text{P}_x)\text{O}$. The rectangle-like spectral shape indicates a commensurate AFM order. Solid curve is the simulation at $T=4.2$ K. (b) T dependences of $^{31}\text{H}_{\text{int}}$ that is proportional to M_{AFM} and of $(1/T_1T)$ at $x=0.6$. Both results point to the emergence of AFM-2 with $T_N=35$ K. (c) x dependence of ^{31}P -NMR spectra at $T=1.9$ K and (d) T dependences of full-width at half maximum (FWHM) for each x , which provide evidence of AFM-2 occurring at $0.4 \leq x \leq 0.7$ but not at $x=0.3$ or 0.8 .

by assuming the hyperfine-coupling constant at the ^{75}As site, $^{75}\text{A}_{\text{hf}} = 2.0 \sim 2.5$ T/ μ_B in LaFeAsO ,¹⁴ and the ratio $^{75}\text{A}_{\text{hf}}/^{31}\text{A}_{\text{hf}} = ^{75}\text{H}_{\text{int}}/^{31}\text{H}_{\text{int}} = 3.05$ in $(\text{Ca}_4\text{Al}_2\text{O}_6)\text{Fe}_2(\text{As,P})_2$.¹² As shown in Fig. 1(b), $^{31}\text{H}_{\text{int}}(T)$ that is proportional to M_{AFM} develops upon cooling below $T_N=35$ K according to a mean-field type of T dependence. The onset of AFM order is also corroborated by the peak in $(1/T_1T)$ at $T_N=35$ K. Note that $M_{\text{AFM}} \sim 0.18\mu_B$ and $T_N=35$ K for the $x=0.6$ compound are smaller than $M_{\text{AFM}}=0.63^{16} \sim 0.8\mu_B^{17}$ and much lower than $T_N=140$ K for the AFM compound $\text{LaFeAsO}(x=0)$, respectively.

Figure 1(c) shows the x dependence of the ^{31}P -NMR spectrum at low temperatures. The ^{31}P -NMR spectra for $x=0.4, 0.5$, and 0.7 except $x=0.6$ are not rectangular even at 1.9 K, pointing to an inevitable distribution of M_{AFM} . Concomitantly, the peak in $(1/T_1T)$ at approximately T_N is broader for these compounds than for the $x=0.6$ compound [see Fig. 3(b)]. These results are indicative of some homogeneity of T_N in association with an inevitable distribution of P content in the sample as noted in a previous report for $x=0.5$.¹⁸ In this context, the spatially averaged T_N is tentatively evaluated as the temperature below which the full-width at half maximum (FWHM) of each spectrum rapidly increases as shown in Fig. 1(d). On the other hand, the spectra for $x=0.3$ and 0.8 do not undergo such significant broadening even at low temperatures, providing evidence that both are in a

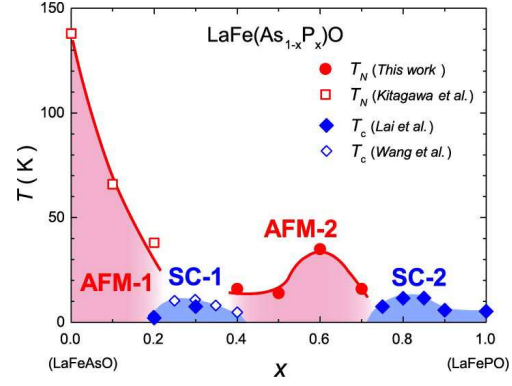


Fig. 2. (Color online) Phase diagram of $\text{LaFe}(\text{As}_{1-x}\text{P}_x)\text{O}$ against x in which the re-emergent AFM-2 intervenes between the SC-1 at $x < 0.4$ (Wang *et al.*¹⁹) and the SC-2 at $0.7 < x$ (Lai *et al.*¹¹).

paramagnetic state. The unexpected onset of AFM-2 at $0.4 \leq x \leq 0.7$ is discontinuous from the AFM-1 emerging at $x \leq 0.2$.¹⁸ As a result, a novel phase diagram of $\text{LaFe}(\text{As}_{1-x}\text{P}_x)\text{O}$ is summarized in Fig. 2, in which the re-emergent AFM-2 intervenes between the SC-1 at $0.2 < x \leq 0.4$ ¹⁹ and the SC-2 at $0.7 < x$.¹¹

Here, we focus on a possible P-derived evolution of the electronic state in $\text{LaFe}(\text{As}_{1-x}\text{P}_x)\text{O}$. The respective T dependences of the Knight shift K and $(1/T_1T)$ are shown in Figs. 3(a) and 3(b), respectively. The Knight shift comprises the T -dependent spin shift $K_s(T)$ and the T -independent chemical shift K_{chem} . $K_s(T)$ is given by $K_s(T) \propto ^{31}\text{A}_{\text{hf}}\chi_0 \propto ^{31}\text{A}_{\text{hf}}N(E_F)$, using the static spin susceptibility χ_0 and the density of states (DOS) $N(E_F)$ at the Fermi level E_F . In nonmagnetic compounds, it is anticipated that $K_s(T)$ is proportional to $(1/T_1T)^{1/2}$, since Korringa's relation $(1/T_1T) \propto N(E_F)^2$ holds. The plot of $(1/T_1T)^{1/2}$ vs K at $T=200$ K in Fig. 3(c) is close to the linear relation $(1/T_1T)^{1/2} = K_{\text{chem}} + K_s(T)$ with $K_{\text{chem}} \sim 0.03$ (± 0.01)%. Figure 4(a) shows $K_s(T)$ ($= K - K_{\text{chem}}$) for each x . For compounds at x lower than 0.4 , $K_s(T)$ decreases upon cooling as in $\text{LaFeAs}(\text{O,F})$ compounds.^{10,20,21} This is because the Fermi level is on the tail of the large peak of the DOS beneath E_F .^{22,23} However, in the intermediate x range of $0.4 \leq x \leq 0.7$, once $K_s(T)$ increases in the high-temperature range, it then decreases toward $T=0$. At x higher than 0.8 , $K_s(T)$ monotonically increases upon cooling, suggesting the appearance of a sharp peak of DOS just at E_F .

The band calculation has revealed that the Fermi surface (FS) of LaFeAsO is composed of two hole FSs at $\Gamma(0,0)$, one small hole FS at $\Gamma'(\pi,\pi)$, and two electron FSs at $M[(\pi,0),(0,\pi)]$ in the unfolded FS regime; these nearly cylindrical FSs can be connected by the interband nesting vector Q .^{24,25} When the pnictogen height is as small as that in LaFePO , the Γ' mainly originating from the $d_{X^2-Y^2}$ orbit sinks below E_F , although the two nearly cylindrical hole FSs at Γ and the two electron FSs at M are maintained. On the other hand, a three-dimensional hole FS around $Z(\pi,\pi,\pi)$ arises from the $d_{3z^2-r^2}$ orbit, which brings about a sharp peak in the DOS just at E_F .^{22,26} As shown in the broken curves in Figs. 3(a) and 4(a), the T dependence of $K_s(T)$ at

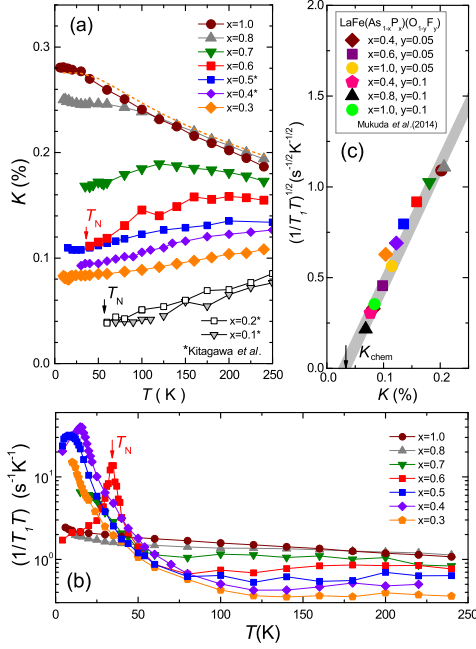


Fig. 3. (Color online) T dependences of (a) Knight shift (K) and (b) $(1/T_1T)$ for $\text{LaFe}(\text{As}_{1-x}\text{P}_x)\text{O}$. (c) Plot of $(1/T_1T)^{1/2}$ vs K at $T=200$ K. The thick line shows the linear relation $(1/T_1T)^{1/2} = K_{\text{chem}} + K_s(T)$ with $K_{\text{chem}} \sim 0.03(\pm 0.01)\%$. Some Knight shift data in (a) are cited from Ref. 18.

$x=1.0$ can be reproduced by assuming the DOS calculated using the band structure of LaFePO .²² To elucidate the appearance of such a characteristic band structure of LaFePO , we deal with $K_s(T \rightarrow 0)$ estimated by extrapolation to $T=0$ in the paramagnetic state above T_N or T_c . As shown in Figs. 4(a) and 4(b), $K_s(T \rightarrow 0)$ increases markedly at $x > 0.7 \sim 0.8$, regardless of the monotonic variation in the lattice parameters.¹¹ Accordingly, we remark that the electronic structure of $\text{LaFe}(\text{As}_{1-x}\text{P}_x)\text{O}$ markedly evolves at approximately $x=0.7 \sim 0.8$. Note that this evolution takes place very close to the x where AFM-2 disappears. This result suggests that the appearance of a $d_{3Z^2-r^2}$ -derived three-dimensional hole pocket causes AFM-2 to be unfavorable, in association with the possible collapse of the nearly two-dimensional LaFeAsO -like band configuration.

Furthermore, it is noteworthy that electron doping through F^- substitution for O^{2-} in $\text{LaFeP}(\text{O}_{1-y}\text{F}_y)$ causes $K_s(T \rightarrow 0)$ to decrease markedly,¹⁰ as shown in Figs. 4(a) and 4(b). This means that doping electrons into LaFePO forces the large DOS at E_F to shift. When noting that the T_c of $\text{LaFeP}(\text{O}_{1-y}\text{F}_y)$ does not vary much, even though this large DOS originating from the $d_{3Z^2-r^2}$ orbit disappears with increasing y , the quasiparticles derived from the hole FS at the Z point have nothing to do with the onset of SC-2. On the other hand, as shown in Fig. 5, $1/T_1T$ at $x=0.8$ and 1.0 increases upon cooling below 50 K even though K_s^2 becomes nearly T -independent in this T range, demonstrating that the subtle evolution of AFMSFs at a finite Q is present in other minority bands in SC-2. Taking the result of the band calculation into account, we suggest that the quasipar-

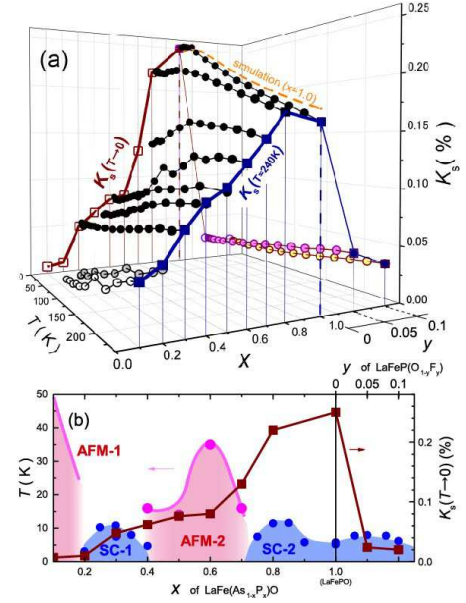


Fig. 4. (Color online) (a) Systematic T dependences of $K_s(T)$ for each x for $\text{LaFe}(\text{As}_{1-x}\text{P}_x)\text{O}$ and $\text{LaFeP}(\text{O}_{1-y}\text{F}_y)$,¹⁰ along with the x dependences of $K_s(T=240$ K) and $K_s(T \rightarrow 0)$ estimated by extrapolation to $T=0$ in the paramagnetic state above T_N or T_c . (b) Plot of $K_s(T \rightarrow 0)$ in the phase diagram.^{9,19,27} Note that $K_s(T \rightarrow 0)$ increases markedly at $x = 0.7 \sim 0.8$, but electron doping through F^- substitution in $\text{LaFeP}(\text{O}_{1-y}\text{F}_y)$ causes $K_s(T \rightarrow 0)$ to decrease markedly.¹⁰ The appearance of a sharp peak of DOS is due to the $d_{3Z^2-r^2}$ orbit for $0.7 \sim 0.8 < x$.

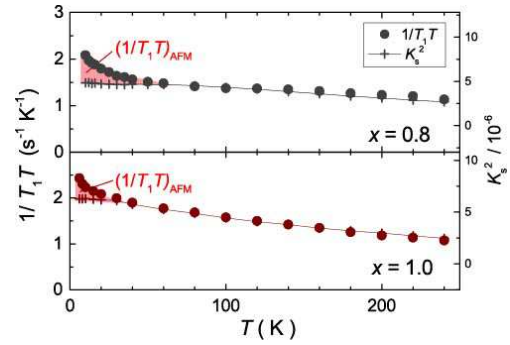


Fig. 5. (Color online) Evaluation of AFMSFs for $x=0.8$ and 1.0 in SC-2. The $1/T_1T$ of these compounds increases upon cooling below 50 K even though K_s^2 becomes nearly T -independent; hence the hatched area denoted as $(1/T_1T)_{\text{AFM}}$ corresponds to the component of $1/T_1T$ due to interband scattering process, i. e., AFMSFs at a finite Q .

ticles originating from the d_{XZ}/d_{YZ} -derived nearly two-dimensional minority bands are responsible for the SC-2 with a relatively low T_c . In this context, this tendency between the onset of T_c and the diversity of the band structure is indicative of the multiband nature observed in Fe-pnictide SC in general.

Finally, we deal with some differences of AFM-1 and AFM-2 in $\text{LaFe}(\text{As}_{1-x}\text{P}_x)\text{O}$. The AFM-1 of LaFeAsO at $x=0$ disappears rapidly around $x \sim 0.2$ where h_{PN} is approximately 1.29 \AA , which coincides with that at the border between the AFM and SC phases observed in many Fe pnictides in the Fe^{2+} -like state with nei-

ther electron nor hole doping.¹² AFM-2 appears in the h_{Pn} range of 1.2~1.25 Å, which is smaller than 1.29 Å. From the recent band calculation, Kuroki *et al.* suggested that FS nesting at bands mainly composed of d_{XZ}/d_{YZ} orbitals becomes better again at the intermediate x of $\text{LaFe}(\text{As}_{1-x}\text{P}_x)\text{O}$,²⁸ consistent with the experimental results. From other context, the reason why the compound $\text{LaFe}(\text{As}_{1-x}\text{P}_x)(\text{O}_{0.95}\text{F}_{0.05})$ with $x=0.6$ exhibits a maximum $T_c=24$ K against x is found, that is, the marked enhancement of AFMSFs at low energies as a result of the depression of AFM-2 by electron doping.¹⁰ Eventually, interband nesting on d_{XZ}/d_{YZ} orbitals must be a key factor for the emergence of SC around AFM-2.

However, note that AFMSFs at low energies are not always highly significant in Fe pnictide compounds with $T_c > 50$ K.²⁹ Recently, another type of stripe AFM(H) phase carrying a large AFM moment but exhibiting a low T_N has been reported for heavily electron-doped compounds $\text{LaFeAs}(\text{O},\text{H})$.³⁰ These electronic states undergoing a novel structural deformation are totally different from those of the mother compound with AFM-1 order.³¹ It has been reported that the SC(H) in $\text{LaFeAs}(\text{O},\text{H})$ that exhibits a T_c higher than in SC-1 occurs owing to the development of AFMSFs at high energies in the vicinity of the AFM(H) phase despite the FS nesting condition being significantly worse.³² In this point, the origins of the AFM and SC phases are yet unresolved underlying issues in LaFeAsO -based compounds, which should be clarified through a unified picture in the near future.

In summary, the present ³¹P-NMR studies of $\text{LaFe}(\text{As}_{1-x}\text{P}_x)\text{O}$ have unraveled the re-emergence of AFM-2 with a homogeneous moment of $M_{\text{AFM}} \sim 0.18\mu_B$ and $T_N=35$ K at $x=0.6$. It is highlighted that this AFM-2 takes place at $0.4 \leq x < 0.7$, intervening between the SC-1 at $0.2 < x < 0.4$ and the SC-2 at $0.7 < x$. Note that the electronic structure of $\text{LaFe}(\text{As}_{1-x}\text{P}_x)\text{O}$ markedly evolves at $x=0.7 \sim 0.8$ in such a manner that a three-dimensional hole FS around $Z(\pi, \pi, \pi)$ arising from the $d_{3Z^2-r^2}$ orbit brings about a sharp peak in the DOS just at E_F .^{22,26} This result suggests that the appearance of a $d_{3Z^2-r^2}$ -derived three-dimensional hole pocket causes AFM-2 to be unfavorable in association with the collapse of the nearly two-dimensional LaFeAsO -like band configuration. From another context, the reason why the compound $\text{LaFe}(\text{As}_{1-x}\text{P}_x)(\text{O}_{0.95}\text{F}_{0.05})$ with $x=0.6$ exhibits a maximum $T_c=24$ K against x has been found, that is, the marked enhancement of AFMSFs at low energies as a result of the depression of AFM-2 by electron doping.¹⁰ Eventually, interband nesting on d_{XZ}/d_{YZ} orbitals must be a key factor for the emergence of SC around AFM-2.

We thank K. Kuroki, H. Usui, and K. Suzuki for valuable discussion, and K. Ishida for providing us their experimental data in the low x range. This work was supported by KAKENHI from JSPS.

- 1) Y. Kamihara, T. Watanabe, M. Hirano, and H. Hosono, *J. Am. Chem. Soc.* **130**, 3296 (2008).
- 2) Y. Kamihara, H. Hiramatsu, M. Hirano, R. Kawamura, H. Yanagi, T. Kamiya, and H. Hosono, *J. Am. Chem. Soc.* **128**, 10012 (2006).
- 3) Z. A. Ren, W. Lu, J. Yang, W. Yi, X. L. Shen, Z. C. Li, G. C. Che, X. L. Dong, L. L. Sun, F. Zhou, and Z. X. Zhao, *Chin.*

- Phys. Lett.* **25**, 2215 (2008).
- 4) Z. A. Ren, G. C. Che, X. L. Dong, J. Yang, W. Lu, W. Yi, X. L. Shen, Z. C. Li, L. L. Sun, F. Zhou, and Z. X. Zhao, *Europhys. Lett.* **83**, 17002 (2008).
- 5) C. H. Lee, A. Iyo, H. Eisaki, H. Kito, M. T. Fernandez-Diaz, T. Ito, K. Kihou, H. Matsushita, M. Braden, and K. Yamada, *J. Phys. Soc. Jpn.* **77**, 083704 (2008).
- 6) Y. Mizuguchi, Y. Hara, K. Deguchi, S. Tsuda, T. Yamaguchi, K. Takeda, H. Kotegawa, H. Tou, and Y. Takano, *Supercond. Sci. Technol.* **23**, 054013 (2010).
- 7) S. Saijo, S. Suzuki, S. Miyasaka, and S. Tajima, *Physica C* **470**, S298 (2010).
- 8) S. Miyasaka, A. Takemori, T. Kobayashi, S. Suzuki, S. Saijo, and S. Tajima, *J. Phys. Soc. Jpn.* **82**, 124706 (2013).
- 9) K. T. Lai, A. Takemori, S. Miyasaka, S. Tajima, A. Nakao, H. Nakao, R. Kumai, and Y. Murakami, *JPS Conf. Proc.* **1**, 012104 (2014).
- 10) H. Mukuda, F. Engetsu, K. Yamamoto, K. T. Lai, M. Yashima, Y. Kitaoka, A. Takemori, S. Miyasaka, and S. Tajima, *Phys. Rev. B* **89**, 064511 (2014).
- 11) K. T. Lai, A. Takemori, S. Miyasaka, F. Engetsu, H. Mukuda, and S. Tajima, submitted to *Phys. Rev. B*.
- 12) H. Kinouchi, H. Mukuda, Y. Kitaoka, P. M. Shirage, H. Fujihisa, Y. Gotoh, H. Eisaki, and A. Iyo, *Phys. Rev. B* **87**, 121101 (2013).
- 13) K. Kitagawa, N. Katayama, K. Ohgushi, M. Yoshida, and M. Takigawa, *J. Phys. Soc. Jpn.* **77**, 114709 (2008).
- 14) ^{75}As was evaluated from the data of $^{75}\text{H}_{\text{int}} = 1.6 \text{ T}^{15}$ and $M_{\text{AFM}} = 0.63\mu_B^{16} \sim 0.8\mu_B^{17}$ for the AFM ordered LaFeAsO .
- 15) H. Mukuda, N. Terasaki, N. Tamura, H. Kinouchi, M. Yashima, Y. Kitaoka, K. Miyazawa, P. M. Shirage, S. Suzuki, S. Miyasaka, S. Tajima, H. Kito, H. Eisaki, and A. Iyo, *J. Phys. Soc. Jpn.* **78**, 084717 (2009).
- 16) N. Qureshi, Y. Drees, J. Werner, S. Wurmehl, C. Hess, R. Klingeler, B. Büchner, M. T. Fernández-Díaz, and M. Braden, *Phys. Rev. B* **82**, 184521 (2010).
- 17) H.-F. Li, W. Tian, J.-Q. Yan, J. L. Zarestky, R. W. McCallum, T. A. Lograsso, and D. Vaknin, *Phys. Rev. B* **82**, 064409 (2010).
- 18) S. Kitagawa, T. Iye, Y. Nakai, K. Ishida, C. Wang, G. -H. Cao, and Z. -A. Xu, *J. Phys. Soc. Jpn.* **83**, 023707 (2014).
- 19) C. Wang, S. Jiang, Q. Tao, Z. Ren, Y. Li, L. Li, C. Feng, J. Dai, G. Cao, and Z. Xu, *Europhys. Lett.* **86**, 47002 (2009).
- 20) H.-J. Grafe, D. Paar, G. Lang, N. J. Curro, G. Behr, J. Werner, J. Hamann-Berrero, C. Hess, N. Leps, R. Klingeler, and B. Büchner, *Phys. Rev. Lett.* **101**, 047003 (2008).
- 21) N. Terasaki, H. Mukuda, M. Yashima, Y. Kitaoka, K. Miyazawa, P.M. Shirage, H. Kito, H. Eisaki, and A. Iyo, *J. Phys. Soc. Jpn.* **78**, 013701 (2009).
- 22) T. Miyake, T. Kosugi, S. Ishibashi, and K. Terakura, *J. Phys. Soc. Jpn.* **79**, 123713 (2010).
- 23) H. Ikeda, *J. Phys. Soc. Jpn.* **77**, 123707 (2008).
- 24) V. Vildosola, L. Pourovskii, R. Arita, S. Biermann, and A. Georges, *Phys. Rev. B* **78**, 064518 (2008).
- 25) K. Kuroki, H. Usui, S. Onari, R. Arita, and H. Aoki, *Phys. Rev. B* **79**, 224511 (2009).
- 26) S. Lebegue, *Phys. Rev. B* **75**, 035110 (2007).
- 27) T. Okuda, W. Hirata, A. Takemori, S. Suzuki, S. Saijo, S. Miyasaka, and S. Tajima, *J. Phys. Soc. Jpn.* **80**, 044704 (2011).
- 28) K. Kuroki *et al.*, private communication.
- 29) H. Mukuda, S. Furukawa, H. Kinouchi, M. Yashima, Y. Kitaoka, P. M. Shirage, H. Eisaki, and A. Iyo, *Phys. Rev. Lett.* **109**, 157001 (2012).
- 30) M. Hiraiishi, S. Iimura, K. M. Kojima, J. Yamaura, H. Hiraka, K. Ikeda, P. Miao, Y. Ishikawa, S. Torii, M. Miyazaki, I. Yamauchi, A. Koda, K. Ishii, M. Yoshida, J. Mizuki, R. Kadono, R. Kumai, T. Kamiyama, T. Otomo, Y. Murakami, S. Matsuishi, and H. Hosono, *Nat. Phys.* **10**, 300 (2014).
- 31) S. Iimura, S. Matsuishi, H. Sato, T. Hanna, Y. Muraba, S. W. Kim, J. E. Kim, M. Takata and H. Hosono, *Nat. Commun.* **3**, 943 (2012).
- 32) K. Suzuki, H. Usui, K. Kuroki, S. Iimura, Y. Sato, S. Matsuishi, and H. Hosono, *J. Phys. Soc. Jpn.* **82**, 083702 (2013).